Astron. & Astrophys. 48, 1–10 (1976)

The Relation of Galactic Radio Spurs to Spiral Arms

Yoshiaki Sofue
Department of Physics, Nagoya University, Chikusa, Nagoya, Japan

Received November 11, 1975

Summary. An isophotal map is constructed for the brightness distribution of the galactic radio continuum background on the assumption that nonthermal radio-emission is enhanced in space up to ~1 kpc above the spiral arms. The model map agrees well with observed maps in many characteristics, particularly in the galactic spurs. The existence of Loops II and III is doubtful; they appear to be the result of superpositions of numerous spurs along the spiral arms.
Detailed inspection of the observed radio maps reveals a systematic inclination of spur-ridges by 20–30° toward anticenter sides in the inner region of the Galaxy. The inclination suggests some horizontal force on the inner spurs. The force might be the result of the dynamical pressure of a galactic wind or a horizontal stream of gas blowing in the halo. The spurs might therefore be promising probes for investigating the dynamical structure of the galactic gaseous halo.

Key words: the Galaxy — galactic halo — radio spurs — spiral arms

I. Introduction

Galactic spurs in the radio continuum have been widely assumed to be faint supernova remnants (SNR) with extremely large diameters (Hanbury Brown *et al.*, 1960; Oda and Hasegawa, 1962; Haslam *et al.*, 1971; Berkhuijsen *et al.*, 1971; Spoelstra, 1972). The SNR hypothesis has been based primarily on loop features of a few spur ridges which lie on small circles on the sky (Quigley and Haslam, 1965). Four loops have been so far identified; Loops I–IV.
Recently, we have proposed that the spurs are due to tengential views of bank-shaped radio-emitting regions ("non-thermal banks") above spiral arms and also above interarm links or fins in our Galaxy (Sofue, 1973; Sofue *et al.*, 1974; Fujimoto *et al.*, 1975: these are henceforth referred to as Papers I, II and III, respectively). The nonthermal banks are considered to be produced by successive inflations of magnetic fields and cosmic rays (Parker, 1969) out of the gaseous arms associated with galactic shock waves (Fujimoto, 1966; Roberts, 1969; Roberts and Yuan, 1970; Tosa, 1973).
In the present paper, we reexamine in more detail the galactic shock (GS) hypothesis with special reference to radio continuum emission. We construct a radio map on the basis of the GS hypothesis and using a more realistic model of the galactic spiral structure than that adopted in Paper I.
Recently, Haslam *et al.* (1974) carried out a further survey of the radio background at 408 MHz. From their brightness distribution map, we can investigate finer radio structure of the Galaxy, in particular galactic spurs in the inner region of the solar circle. We examine the distribution and orientation of the inner spurs, and briefly discuss their interactions with gas in the galactic halo. The spurs might be interpreted as probes (or windfurnace-gauges) to investigate the dynamical structure of the gaseous halo.

II. Radio Spurs and H I Spiral Arms

In Paper I, we constructed some model contour-maps of the galactic radio background on the basis of the GS hypothesis. In this hypothesis, nonthermal bank-shaped halos are assumed to be produced above the spiral arms by inflations of both magnetic fields and cosmic rays out of the galactic shocked regions. In that paper, we used bisymmetric Archimedes spirals determined by Mills (1959) as a basic geometry for the spiral arms. However, the model spirals were so simplified that it was difficult to reproduce some of characteristic features observed in the outer region of the solar circle.
In the present paper, instead, we adopt a more realistic model of the Galaxy derived from the H I-line observations at wavelength of 21-cm. On the basis of the H I arms, we compose a radio map of continuum emission of the Galaxy. We compare the model map with the observed maps, and discuss the background features with special regard to the spurs.

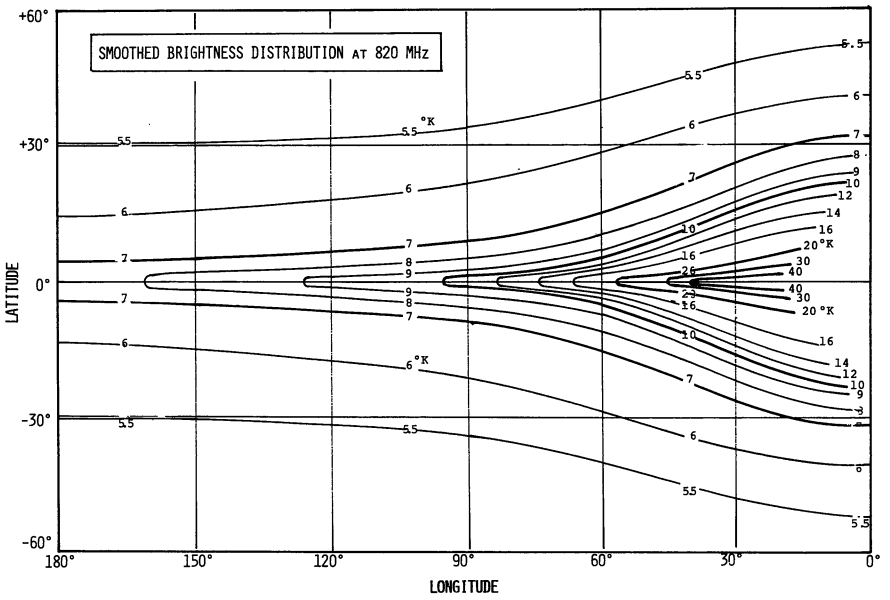

Fig. 1a. The smooth distribution of brightness temperature at 820 MHz of the Galaxy, or, the "flat component". This was obtained after a subtraction of irregular enhancements like spurs from the observed brightness distribution (Berkhuijsen, 1972)

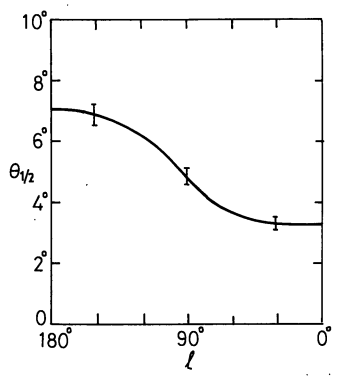

Fig. 1b. Angular half-thickness $\theta_{1/2}$ of the radio disk of the Galaxy, measured from the flat component in Fig. 1a. Typical error bars are indicated

(i) Flat Component of the Galactic Background Emission

We begin with separation of the overall flat component and locally enhanced components observed as radio spurs in the continuum background. For this purpose, we plotted the brightness temperature at 820 MHz observed by Berkhuijsen (1972) against the longitude at a fixed latitude. We then drew a smooth line to fit the lower envelope of the plot. Such smooth lines were obtained for wide range of latitude. Figure 1a shows the smooth map of the flat component of our Galaxy at 820 MHz obtained by use of the lines.

From the flat component obtained here, we can get some information about the typical thickness of the radio disk of our Galaxy. In Fig. 1b we plot angular half-thickness of the flat component $\theta_{1/2}$ read from Fig. 1a as a function of the longitude. Here the angle $\theta_{1/2}$ is defined as a latitude at which the brightness corrected for the uniform component of 5 °K decreases to a half of that at the galactic equator. This figure indicates that the half-thickness in the direction of the galactic center is 3.3°. This corresponds to a characteristic half-width of the radio disk $z_{1/2}=580$ pc, if the line-of-sight depth is 10 kpc. Similarly, in the anticenter direction, we have $\theta_{1/2}=7°$ corresponding to $z_{1/2}=610$ pc, if the line-of-sight depth is 5 kpc.

The flat component includes thermal emission from H II regions distributed close to the galactic plane. This implies that, when the nonthermal emission alone is concerned, the brightness temperature near the galactic equator would be overestimated. We should, therefore, regard the above values as lower limits for the thickness of the nonthermal radio disk.

Hence we may conclude that the nonthermal radio emission of the Galaxy has a typical half-thickness of $z_{1/2}\geqq 600$ pc. This result is in a good agreement with the observation of an extragalactic edge-on galaxy at 408 MHz by Pooley (1969). The half-thickness of the thermal electron disk of our Galaxy has also been estimated to be between 400 and 1000 pc (Falgarone and Lequeux, 1973). These values are comparable with the z-extension of the spurs ($z=1.2$ kpc) adopted below.

(ii) Spur Component Predicted from the GS *Hypothesis*

As in Paper I, we assume that the radio emission is enhanced in the nonthermal bank which extends vertically up to $z\sim 1$ kpc from the arm. For simplicity, the enhancement in the radio emissivity is assumed to be constant up to 1.2 kpc in the z-direction and pro-

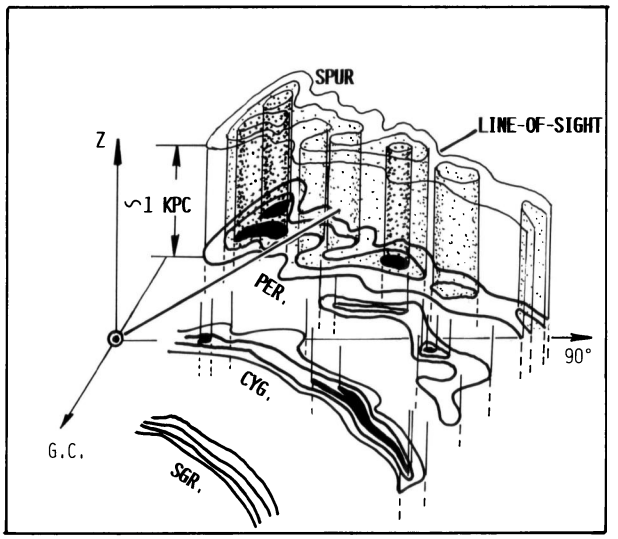

Fig. 2a. Schematic illustration of "nonthermal banks", or radio emitting regions assumed to be responsible for the spurs. They are assumed to extend ~1 kpc vertically from the H I-gas arms

portional to the H I-gas density at the galactic plane. Above $z=1.2$ kpc, the excess emissivity is assumed to be zero (Fig. 2).

We use the H I-map presented by Westerhout (1957) in which are given both the density distribution of H I gas projected onto the galactic plane and z-displacement of the gaseous sheet from the plane. We define the arms as regions where the density is higher than 0.6 cm^{-3} on the map. In the inner region of the solar circle, the H I gas is distributed close to the galactic plane, whereas in the outer region there is a significant displacement of the sheet from the equatorial plane. We also take account of this bending of the outer portion.

We then compute excess brightness temperature responsible for the spur component through integration of the enhancement of the emissivity in the nonthermal banks along a line-of-sight. In order to avoid a contribution from the uncertain distribution of gas near the sun, the integrations excluded the local region within 1 kpc of the sun. Figure 2a illustrates the model distribution of the radio banks of enhanced emissivity. Figure 2b shows their cross sections at a few longitudes. The brightness was obtained at every 2.5–5° interval of longitude and at 2° of latitude.

Here the unit of the computed brightness is yet arbitrary. We then calculate the ratios of the computed brightness to the observed excess brightness over the smooth background at several points at $l=60$–$160°$, $b=20$–$30°$. We take an average of the ratios, and use it as a normalization factor for the computed brightness. Fig. 3a shows the distribution of the brightness temperature at 820 MHz for the outer spur components at $l=80°$–$170°$, and Fig. 3b shows that for the inner spur components at $l \leqq 80°$.

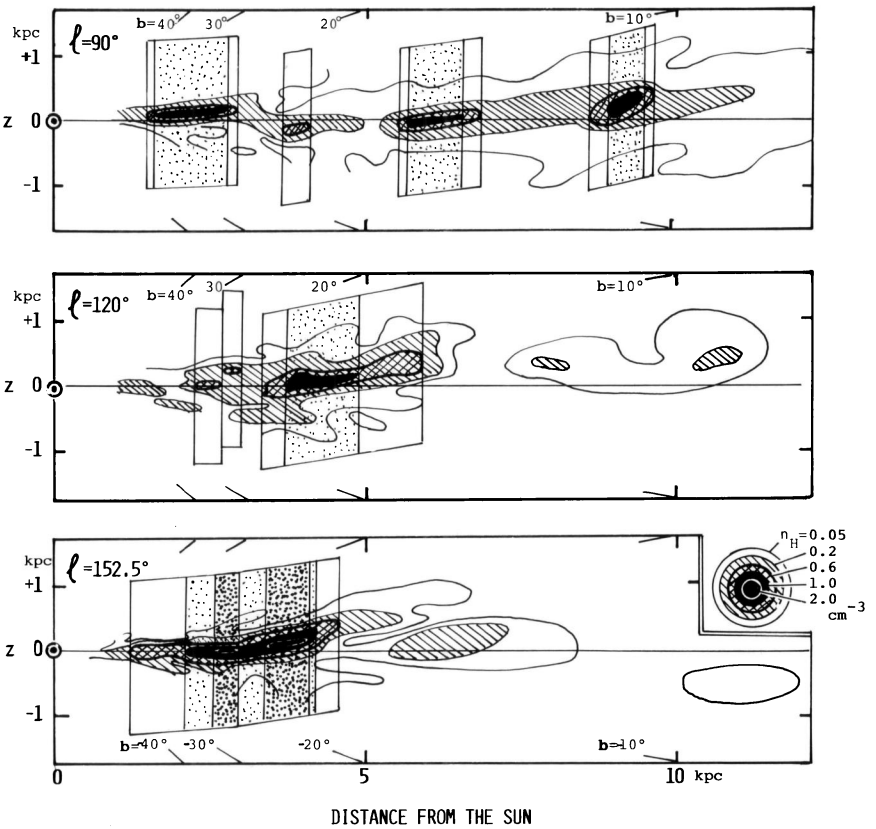

Fig. 2b. Cross sections of the H I-arms and of nonthermal banks at $l=90°$, 120° and 152.5°. The H I-gas distribution is due to Westerhout (1957)

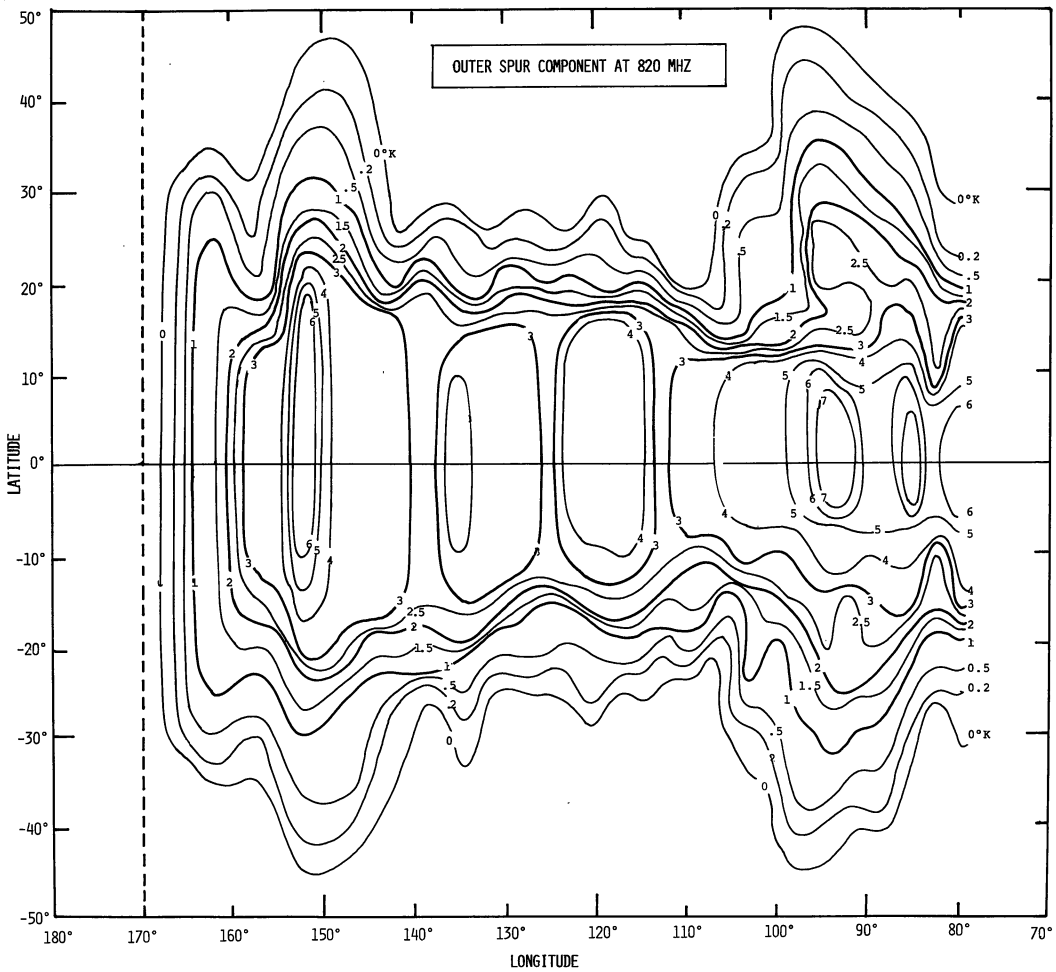

Fig. 3a. Outer model spur-component ($l = 80°$ to $170°$) predicted from the assumption that nonthermal emission is enhanced above the spiral arms as shown in Fig. 2. The brightness temperature was obtained by normalizing the mean excess in the observed brightness over that in the flat component at $l = 90$–$160°$, $b = 20$–$30°$

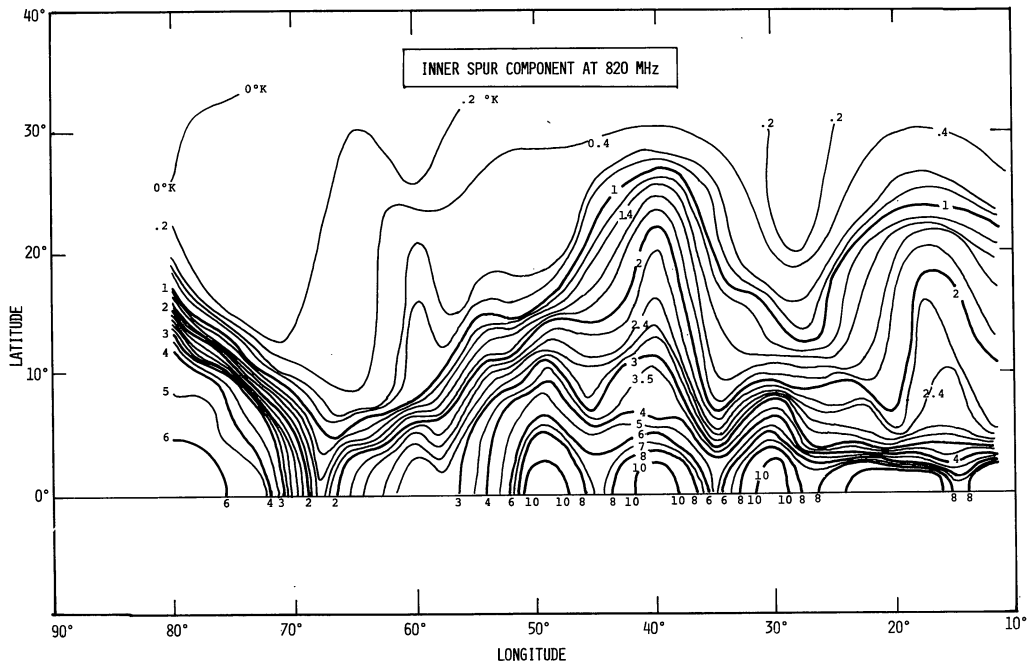

Fig. 3b. The same as Fig. 3a, but for inner model spur-component

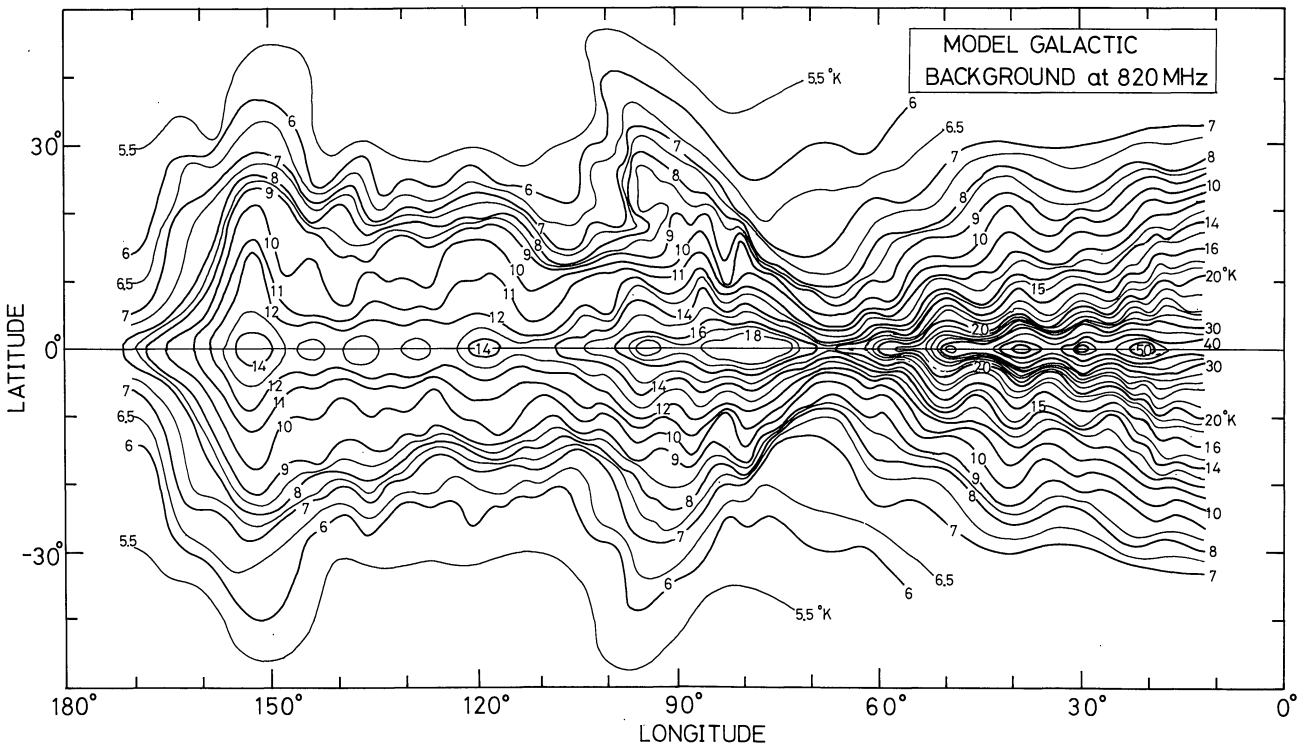

Fig. 4. Model isophotal map of the "galactic" background at 820 MHz formed by a superposition of Fig. 3 on Fig. 1. The spurs, humps, steps and valleys of contour lines are in good agreement with the observations (Fig. 5)

The normalization procedure enables us to estimate an absolute emissivity in the spur region. For example, at $l=90°$, $b=20°$, the excess temperature due to the spur component is 2° K at 820 MHz. It corresponds to an emissivity of $\varepsilon=2kv^2T_b/Lc^2=1.2\times10^{-40}$ erg cm^{-3} s^{-1} Hz^{-1}, when the depth L is taken as 1 kpc (Fig. 2b). If we assume that the spectrum of cosmic-ray electrons is $N(E)=N_e^{-\gamma}$ cm^{-2}s^{-1}sterad^{-1}Gev^{-1} with $N_e=8\times10^{-3}$ and $\gamma=2.4$ (Okuda and Tanaka, 1968), we have $B=2\times10^{-6}$ Gauss as the field strength of the component perpendicular to the line of sight. Here T_b is the excess brightness temperature, v is the frequency, and E is the energy of a cosmic ray electron. Further discussion of the radio emissivity, magnetic fields and cosmic rays in the spur regions is given in Fujimoto *et al.* (1975).

(iii) Model Isophotal Map of the Galactic Background Emission

We superpose the spur component in Fig. 3 on the flat component in Fig. 1. Figure 4 displays the composite map of the "galactic emission" at 820 MHz. For comparison, we show in Fig. 5 the 820 MHz map made by Berkhuijsen (1972). We also display the distribution of H I gas projected onto the galactic plane as derived from 21-cm line observations (Westerhout, 1957). In this figure are indicated some conceivable relations among prominent spurs and their directions to the corresponding spiral arms and H I-regions.

III. Comparison of the Model Isophotes with Observations

We now compare the model map with the observations, and discuss some characteristic features of the radio continuum background with special regard to the spurs.

(i) Comparison

There is a remarkable similarity between Figs. 4 and 5 in many prominent features such as spurs and humps of the contour lines. The reproduction of observed features is here much improved over that obtained in Paper I. Some typical features seen in these figures are discussed below.

(a) Perseus Spurs at $l=150°$. These spurs have ridge lines almost symmetrically stretching from $(l, b)=$ (150°, 10°) to (150°, 50°), and from (150°, −10°), to (150°, −50°) in Fig. 5. They are well reproduced by the present model in Fig. 4. These two spurs are formed mainly from radio emission above and below the compressed H I regions in the Persus Arm as indicated with dark areas at $l=140°$–$150°$ on the H I map in Fig. 5.

(b) Perseus Hump at $l=110$–$130°$. This is observed as a wide hump of contour lines at $l=110$–$130°$ at positive latitudes. Tosa and Sofue (1974) and Sofue and Tosa (1974) have shown that this hump is associated with the

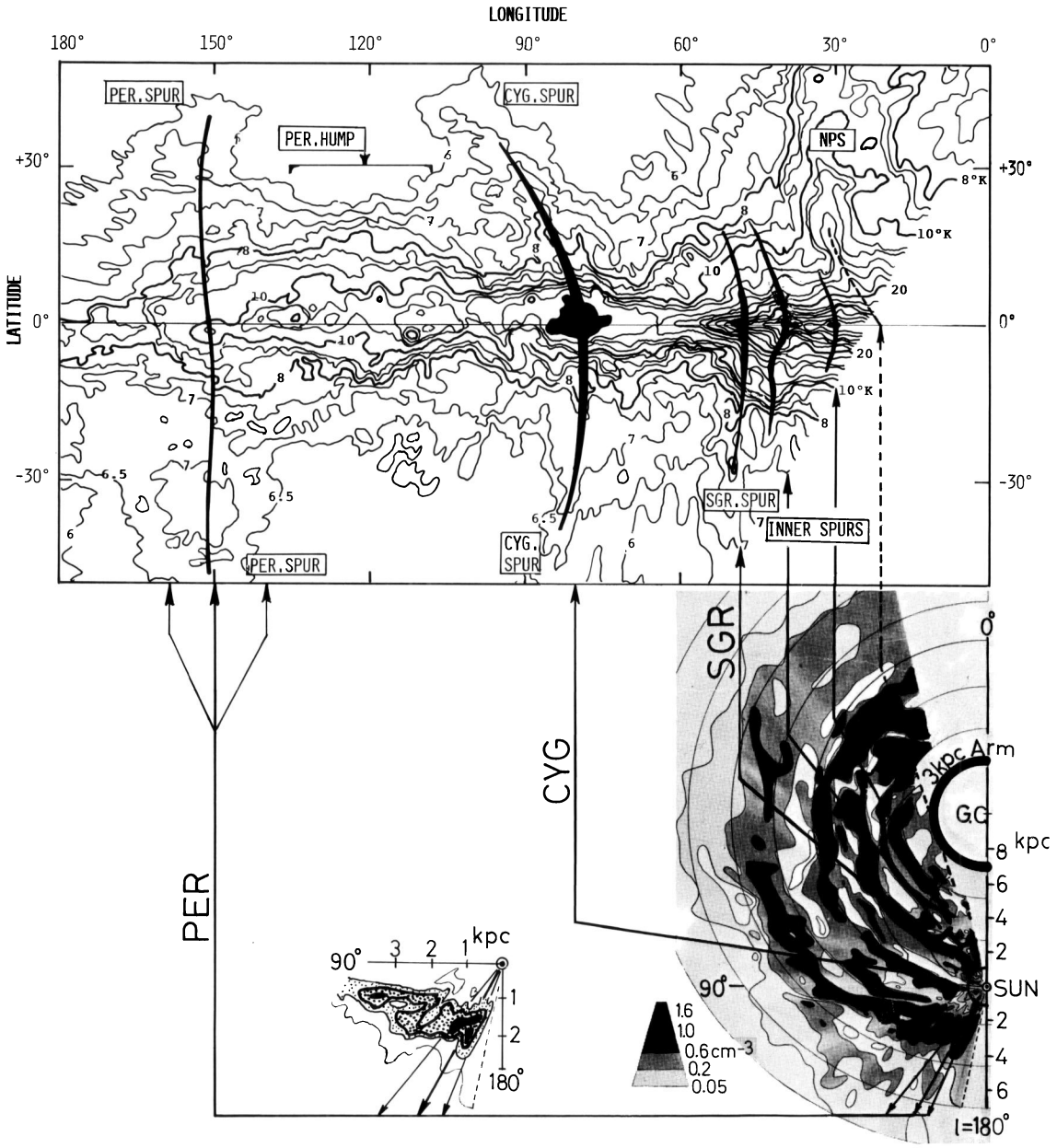

Fig. 5. Observed radio brightness at 820 MHz (Berkhuijsen, 1972), and H I-gas distribution projected onto the galactic plane (Westerhout, 1957). Positional relations among radio spurs and tangential directions of the spiral arms are indicated with thick lines. Also indicated is the relation of the Perseus Spurs at $l=150°$ to the high codensations of H I-gas around $l=150°$ in the Perseus arm. (Compare with Fig. 4.) Note that smooth extension of the North Polar Spur ridge crosses the galactic plane at $l=21°$, which exactly coincides with the tangential direction of the 3 kpc arm

"Perseus complex region" where are concentrated H II regions, OB-associations, and open clusters which belong to the Perseus arm. They have shown that this hump is also associated with ascending motions of H I-gas clouds in the z-direction, and the clouds reach heights of 1–2 kpc above the arm.

This hump is well reproduced by the present model as a vertical spread of the radio disk at $l=110$–$130°$. The asymmetry in latitude of the observed hump is also found in the model map: the hump is more pronounced at positive latitudes than at negative latitudes. This asymmetry probably comes from the bending of the Galaxy, the upward displacement of which attains a maximum at $l\cong120°$. Note that the asymmetry in the model (Fig. 4) is somewhat smaller than the observed asymmetry (Fig. 5). This is because we do not take into account the z-displacement of the radio disk reponsible for the flat component.

(c) Cygnus Spurs at $l=80$–$90°$. In the tangential direction to the local arm there are two prominent spurs protruding symmetrically from the Cygnus Region toward positive and negative latitudes. These spurs are well reproduced in the model (Fig. 4), although the model

spur at negative latitudes is somewhat shifted to increasing longitudes compared with the observation. The spur at positive latitudes closely resembles the observed one in shape and configuration. The ridges of the model spurs emerge almost vertically from the galactic plane, eventually bending towards the anti-center sides. Note also that their ridges appear as a large arc, which is the reason that the northern Cygnus Spur has been said to lie on a loop, or Loop III.

The spur at positive latitude looks as if it overhangs the Perseus Hump. This feature is also well reproduced on the model map. The "overhang" comes from the fact that the line-of-sight depth of the emission region has a minimum at $b \approx 20°$ around $l \approx 95°$ (Fig. 2).

The model brightness at $l=80°$, $b=0°$, just in the tangential direction to the Cygnus Arm, appears to be much lower than the observed value. This is because H II regions in the spiral arm are not included in the present model. The same applies to the directions tangential to the inner spiral arms.

(d) Dips of Contours at $l=60$–$70°$. The background emission has a wide minimum at $l=60$–$70°$, which is also reproduced in Fig. 4. This "valley" of brightness is due to lack of H I gas in space between the Cygnus and Sagittarius arms.

(e) Sagittarius Hump. This step-like structure is located at $l=50°$ above and below the tangential direction to the Sagittarius arm, and is fairly well reproduced by the model. It is associated with the Sagittarius Spurs which extend above and below the plane, to $b=\pm 20$–$30°$.

(f) Small Inner Spurs. A variety of small spurs are observed in the inner region of the Galaxy. They apparently protrude from the galactic plane, and are, to a good extent, reproduced in the model. These spurs are discussed further in the next section.

(g) North Polar Spur. In Paper I, we could reproduce this spur by assuming a fin or an interarm-link between the Cygnus and Sagittarius arms. We assumed that the fin stretches by 1–2 kpc from the solar vicinity toward the Sagittarius arm in the direction of $l=30°$. The fin structure was introduced on the basis of the existence of a large region of obscured starlight at $l=20$–$30°$ in the Milky Way. In the present paper, however, we have neglected such local contributions within 1 kpc of the sun, and therefore, the NPS is not reproduced.

(ii) On Galactic Loops

Loops I–IV were identified after Quigley and Haslam (1965) suggested that some ridges of spurs lie on small circles on the sky. The apparent loop features seem to have impressed many investigators to make the SNR hypothesis (see, e.g., Berkhuijsen *et al.*, 1971). A possible relation among the Loops and the spurs is as follows: The northern Perseus Spur is a segment of Loop III, the southern Perseus Spur is on Loop II, the northern Cygnus Spur on Loop III, and the southern Sagittarius Spur is a part of Loop II.

We stress, however, that all of these spurs can be naturally accounted for on the basis of the GS hypothesis: Fewer assumptions are made than in the SNR hypothesis; we need only to assume the nonthermal banks along the spiral arms. With the SNR hypothesis, on the contrary, we must assume some nearby SNRs with extremely large radii, 50–100 pc. These giant SNRs were introduced only in order to explain the loops, with no other independent reason. Furthermore, when such faint and extended objects are concerned, a confusion of the galactic radio emission should be corrected for very carefully: we must discuss "residual" component subtracted from the galactic background. On the other hand, as shown in Figs. 3 and 4, the background itself is far from the smooth distribution shown in Fig. 1, and includes a variety of fluctuations due to the spiral arms and local condensations of gas.

From these arguments, we are inclined to believe that the physical existence of the loop structures, in particular Loops II and III, is very doubtful. It seems better to regard them as being the result of an apparent projection effect of the Perseus, Cygnus, and Sagittarius Spurs. (See also Paper II for several difficulties associated with the spurs and Loops in the SNR hypothesis.)

IV. Inner Spurs and Their Inclinations

(i) Inner Spurs

Berkhuijsen (1971) noted many ridges of contours on her 820 MHz map. She has collected the data about the ridges and discussed their physical meanings with special references to loop structures and the SNR hypothesis. Recently, Haslam *et al.* (1974) presented a further survey at 408 MHz of the background emission at $12\,\mathrm{h} \leqq \mathrm{RA} \leqq 04\,\mathrm{h}$, $-8° \leqq \mathrm{Dec} \leqq +48°$, which includes the galactic plane at $l=20$–$90°$. Their maps, especially the latter, reveal many interesting features of the radio structure of our Galaxy. Particularly conspicuous are many small spurs protruding from the galactic plane in the inner region, $l \lesssim 60°$. These spurs can naturally be attributable to the radio emitting banks located above the inner spiral arms and to some other local condensations of gas in the galactic plane. Most of them can be reproduced by our model as shown in Fig. 4.

A careful inspection of this map (Fig. 6) reveals a remarkable fact that the spurs are not exactly perpendicular to the equatorial plane, but are systematically inclined toward increasing longitudes, or anticenter sides. Such features cannot be attributed merely to the increase of the background brightness toward the galactic center. A similar trend of inclination of the spurs is also seen on the whole-sky map at 150 MHz of Landecker and Wielebinski (1970). From their map,

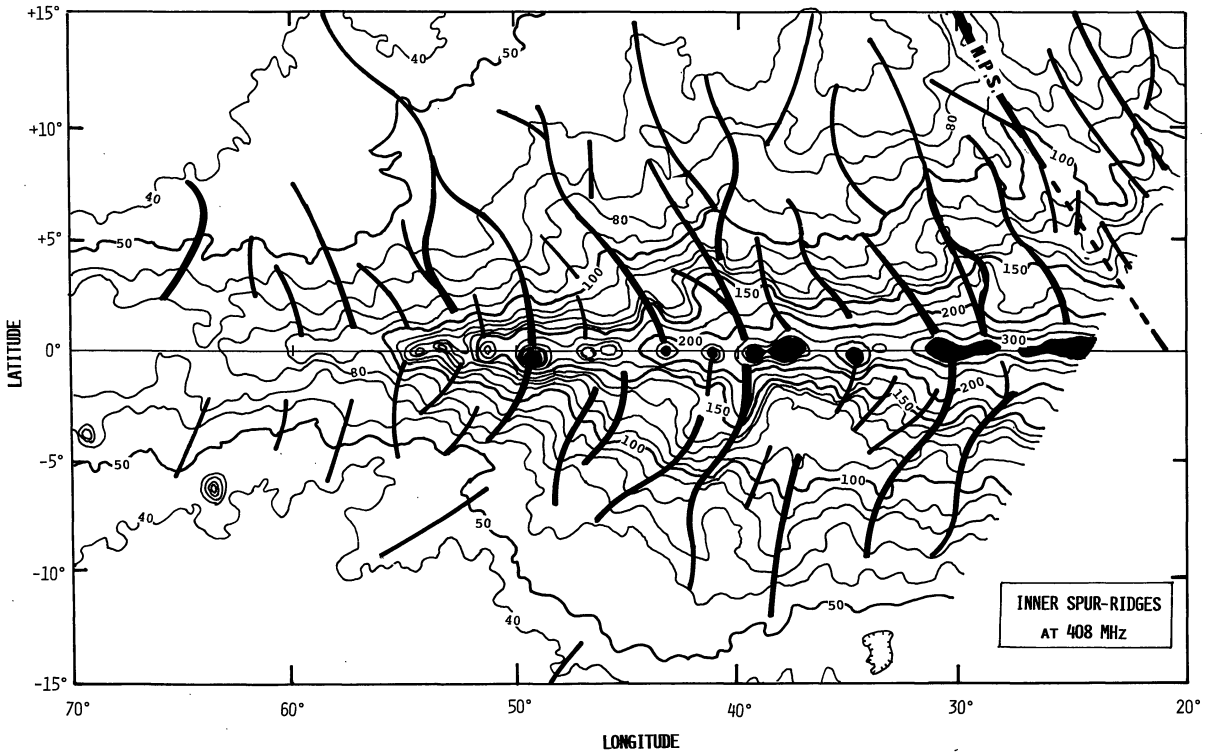

Fig. 6. Inner spur ridges indicated on the 408 MHz map (Haslam *et al.*, 1974). Note the systematic inclination of the spurs toward anticenter sides, which suggests some horizontal force acting on the spurs

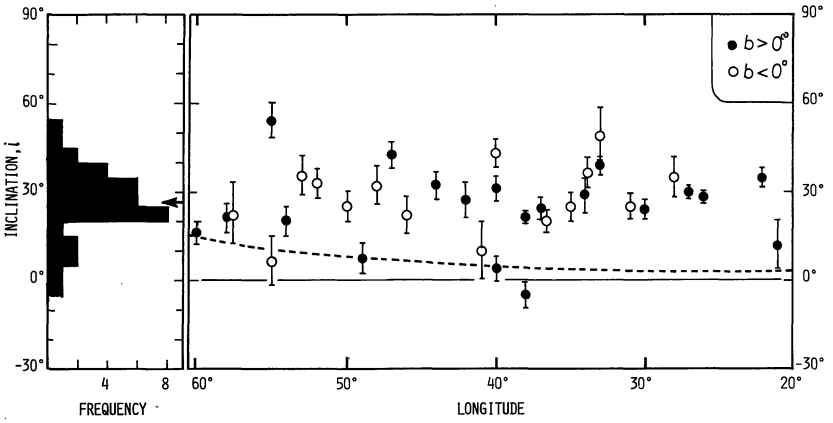

Fig. 7. Inner-spur inclination i plotted against galactic longitude, and their frequency distribution. The frequency has a peak at $i=26°$. Filled circles: inclinations for spurs at $b>0°$; open circles: those for $b<0°$. The error bars are eye-estimates. The dashed line indicates the inclinations of the model spur-ridges (Fig. 4)

we find that ridges at $l=240$–$0°$ are tilted, in turn, toward decreasing longitudes.

Consequently, we may conclude that the galactic spurs are systematically inclined from the perpendicular toward anticenter sides at roughly a constant angle of 20–30°. Figure 6 shows the ridges collected from the map at 408 MHz of Haslam *et al.* (1974). Figure 7 shows a plot of the tilt angles measured from the perpendicular toward the anticenter sides for spurs at $l=20$–$60°$. The frequency distribution of the inclination angles is also indicated. The frequency has a peak at $i=26°$. The dashed line in the figure indicates the inclination of the model spur-ridges read from Fig. 4.

If the emitting regions responsible for the spurs emerge vertically from the galactic plane as is assumed in Section II, no significant inclination could be expected for the inner spurs. Indeed, the inclination for the inner spurs in the model is less than $\sim 5°$ at $l \lesssim 50°$. Hence, this inclination must be caused by some systematic effect intrinsic to the spurs themselves. The inclinations

observed at $l \gtrsim 60°$, on the other hand, are mostly due to a projection effect and are well reproduced by our model.

In this context, it is of interest that the ridge line of the North Polar Spur runs almost parallel to these small spurs, which suggests a common galactic origin for the NPS and these inner spurs.

(ii) Origin of the Spur Inclination

We briefly discuss the cause of the observed inclination of the inner spurs. As already mentioned, the nonthermal banks are considered to be produced by inflations of magnetic fields with cosmic rays as a result of the Parker-type instability. The inflations are enhanced above the gaseous spiral arms associated with the galactic shocked regions.

Unless any non-vertical force acts on the inner spurs, the inflation should take place exactly in the z-direction. The spur ridges at $l \lesssim 50°$ should then appear to be almost perpendicular to the galactic equator. Hence, the fact that the spurs trail toward the anticenter sides might be evidence for some radial force which pushes the banks outward. The force appears to act only in the inner region of the Galaxy.

We suggest three possible explanations for the horizontal force: (i) a galactic wind in the halo blowing horizontally from the central bulge of the Galaxy, or a horizontal gas-stream of galactic scale; (ii) radiation pressure of starlight from the central bulge, acting on dust grains in the banks; (iii) an inclination intrinsic to the spurs when the three-dimensional structure of the galactic shocks is taken into account. The first of these suggestions seems the most promising, though we leave a detailed and quantitative discussion to a separate paper (Sofue *et al.*, 1976).

V. Conclusions

Model Contour Map and the Spurs

On the basis of our galactic shock hypothesis for spurs proposed in Paper I, we have constructed a model map of the radio continuum emission of the Galaxy (Fig. 4). We assumed that the radio emissivity is enhanced in the halo above the spiral arms, or in the radio banks which extend in the z-direction up to ~ 1 kpc. The model map resembles observed radio maps in many respects (Figs. 4 and 5). Most of the prominent spurs are well reproduced by the present model. In particular, the reproduction of the Perseus and Cygnus Spurs is much improved in the present model over that in Paper I.

We have presented only one case, namely, that the height of the nonthermal banks is 1.2 kpc, with a step-function distribution for the emissivity in the z-direction. Adoption of somewhat different values of the height, between ~ 0.8 and ~ 1.5 kpc, would give similar results. Similarly, changing the step function emissivity to a gaussian form with a similar scale-height, would not crucially affect the result.

On the SNR *Hypothesis*

In the SNR hypothesis, the spurs were attributed by various authors to faint, nearby SNRs. For such faint and extended objects, however, we should subtract from the observed brightness the galactic contribution due to the nonthermal halos above the spiral arms. If we apply the subtraction based on our model, the spurs making up Loops II and III mostly disappear. It may be concluded that these Loops are not actual loop- or shell-shaped sources, but are instead a projection effect of the Cygnus, Perseus and Sagittarius Spurs.

The North Polar Spur

In Paper I, we attributed this spur to a local origin such as a fin-structure near the sun, and we obtained a fairly good fit. However, in the present model, the local contribution within 1 kpc of the sun is ignored and the NPS cannot be reproduced.

We suggest another possible explanation for the origin of the NPS: When the ridge of the NPS is smoothly extended to the galactic plane, it crosses the plane at $l = 21°$. This direction exactly coincides with the tangential direction of the 3 kpc arm located at 3.5 kpc from the galactic center (Fig. 5). The very close coincidence might suggest some physical connection of the NPS with the 3 kpc arm. If this is the case, the NPS might be related to galactic center activity.

Inner Spur Inclination

The ridges of inner spurs on the observed radio maps incline systematically toward anticenter sides at an approximately constant angle of 20–30° to the meridional plane. The inclination might be accounted for by the horizontal and outward pressure exerted on the spurs. The pressure might come from a horizontal stream of gas blowing against the spurs from the central region of the Galaxy.

Probing the Halo by Use of the Spurs

If our galactic shock hypothesis is correct, we can use the spurs as probes or "windfurnace-gauges" for studying the hydrodynamics of the galactic halo.

Acknowledgements. The author expresses his hearty thanks to Professor M. Fujimoto and Dr. M. Tosa for their invaluable discussions.

References

Berkhuijsen, E. M. 1971, *Astron. & Astrophys.* **14**, 359
Berkhuijsen, E. M. 1972, *Astron. & Astrophys. Suppl.* **5**, 263
Berkhuijsen, E. M., Haslam, C. G. T., Salter, C. J. 1971, *Astron. & Astrophys.* **14**, 252
Falgarone, E., Lequeux, J. 1973, *Astron. & Astrophys.* **25**, 253

Fujimoto, M. 1966, in *Non Stable Phenomena in Galaxies*, IAU Symp. No. 29, ed. M. Arakeljan (Academy of Sci. of Armenia, USSR), p. 453
Fujimoto, M., Sofue, Y., Hamajima, K. 1975, in preparation
Hanbury Brown, R., Davies, R. D., Hazard, C. 1960, *Observatory* **80**, 191
Haslam, C. G. T., Wilson, W. E., Graham, D. A., Hunt, G. C. 1974, *Astron. & Astrophys. Suppl.* **13**, 359
Landecker, T. L., Wielebinski, R. 1970, *Australian J. Phys.* **16**, 1
Mills, B. Y. 1959, in *Paris Symposium on Radio Astronomy*, IAU Simp. No. 9, ed. R. N. Bracewell (Stanford Univ. Press, California), p. 431
Oda, M., Hasegawa, H. 1962, *Physics Letter* **1**, 239
Okuda, H., Tanaka, Y. 1968, *Bull. Astron. Inst. Neth.* **20**, 129
Parker, E. N. 1969, *Space Sci. Rev.* **9**, 651
Pooley, G. G. 1969, *Monthly Notices Roy. Astron. Soc.* **144**, 143
Quigley, M. J. S., Haslam, C. G. T. 1965, *Nature* **208**, 741
Roberts, W. W. 1969, *Astrophys. J.* **158**, 123
Roberts, W. W., Yuan, C. 1970, *Astrophys. J.* **161**, 887
Sofue, Y. 1973, *Publ. Astron. Soc. Japan* **25**, 207
Sofue, Y., Fujimoto, M., Tosa, M. 1976, *Publ. Astron. Soc. Japan* **28**, No. 2
Sofue, Y., Hamajima, K., Fujimoto, M. 1974, *Publ. Astron. Soc. Japan* **26**, 399
Sofue, Y., Tosa, M. 1974, *Astron. & Astrophys.* **36**, 237
Spoelstra, T. A. Th. 1972, *Astron. & Astrophys.* **21**, 61
Tosa, M. 1973, *Publ. Astron. Soc. Japan* **25**, 191
Tosa, M., Sofue, Y. 1974, *Astron. & Astrophys.* **32**, 461
Westerhout, G. 1957, *Bull. Astron. Inst. Neth.* **13**, 201

Y. Sofue
Department of Physics
Nagoya University
Chikusa, Nagoya 464
Japan